Change Detection and Assessment of Fire-Damaged Concrete Using Terrestrial Laser Scanning

Wallace MUKUPA, Gethin Wyn ROBERTS, Craig Matthew HANCOCK, Khalil AL-MANASIR, China.

Key words: Laser Scanning, Fire-Damaged Concrete, Assessment, Change Detection

SUMMARY

Fire is one of the serious potential hazards to most structures and damage assessment is the first and the most important job for structural safety evaluation of a structure subjected to fire. The extensive use of concrete as a structural material has neccessitated an investigation into more robust and cost-effective techniques for the assessment of fire-damaged concrete using terrestrial laser scanning. Although concrete is known to be a fire resistant structural material, it undergoes severe changes when exposed to elevated temperatures and this can affect the load bearing capacity of structural bearing elements in several ways. Apart from spalling, there can be a permanent loss of strength in the remaining material. In the aftermath of a fire on a structure, various workers get involved in a variety of response and recovery from disaster operations. Furthermore, following a catastrophic failure of a structure after a fire, rescue workers and emergency responders may be required to enter the fire-damaged structure which can be risky and so an assessment method which has the potential to improve safety was investigated.

Within the field of structural and civil engineering, the methods employed in assessing fire-damaged concrete involve both field and laboratory investigations to determine the extent of fire damage in order to design appropriate and cost effective repairs or to decide whether to demolition the structure. Concrete structures show significant loss of strength when heated above 300ºC. This study aimed at investigating whether terrestrial laser scanning can be used to detect fire-damaged concrete using specimens heated up to 1000ºC as it is important to estimate the maximum temperature attained in a fire. The results obtained from the study clearly demonstrated the feasibility of using terrestrial laser scanning to detect fire-damaged concrete via modelling and analysis of laser returned intensity. Laser scanning has emerged as a complementary assessment method of fire-damaged concrete with a couple of advantages in that the whole concrete element can be scanned and an average intensity value over the area concerned can be determined which would represent the whole element overcoming the challenge of some traditional methods where cores are drilled in limited areas. Scanning is rapid with millions of points measured in a few seconds. Laser scanning of the fire-damaged structure can be done from a distance without having to enter the structure and this improves safety. Laser scanning is a non-destructive technique for detecting fire-damaged concrete.

1. INTRODUCTION

Fire is one of the most serious factors affecting the integrity of materials and structures and can cause catastrophic damage. In an event of a fire, there is need to assess the fire-damaged structure so as to ensure safety and devise appropriate repair strategies. Buildings suffer frequent fire events and past research work has shown trends in investigating the effect of fire on a variety of materials. Concrete and concrete structures have been widely investigated, because of their extensive in the construction industry and according to Ingham (2009) concrete structures such as buildings, parking garages, bridges and concrete-lined tunnels are examples of structures that can be damaged by fire.

Although concrete is a non-combustible material and able to retain much of its load-bearing capacity, its chemical, physical and mechanical properties change once exposed to elevated temperatures. The effects of high temperature on the mechanical response of concrete have been investigated since the middle of the twentieth century and is still undergoing up to today (Ergün *et al.,* 2013). To ascertain whether a structure can be repaired rather than demolished after a fire, an assessment of structural integrity must be made since the main objective of fire damage assessment in concrete structures is to provide the information required to evaluate the residual bearing capacity and durability of the structure (Short *et al.,* 2001; Felicetti, 2013). A thorough assessment of a fire-damaged structure involves both on-site and off-site investigations aimed at determining the extent of fire damage so as to design appropriate and cost effective repairs. The assessment process should quantify the degree and extent of damage to structural elements since this will determine the repair costs (Gosin *et al.,* 2008). Normally, an assessment would usually be used to directly assess the quality and condition of structural members by a combination of the methods such as visual inspection, hammer soundings, ultrasonic testing, breakout drilling, compressive strength tests and petrographic examinations (Ingham, 2009; Short *et al.,* 2001).

Concrete is a composite material produced from aggregate, cement, and water. Therefore, the type and properties of aggregate also play an important role on the properties of concrete exposed to elevated temperatures. The strength degradations of concretes with different aggregates are not same under high temperatures. This is attributed to the mineral structure of the aggregates (Arioz, 2007). Heating of concrete in a fire causes a progressive series of mineralogical and strength changes and details can be found in Ingham (2009). It has has been reported that concrete starts to undergo loss in compressive strength when heated between 200°C and 250°C (Ergün *et al.,* 2013).

Detecting fire-damaged concrete using laser scanning is a new area of research and only a preliminary study involving visual inspection were carried out in Hancock *et al.* (2012). This research adds a new dimension to an investigation into the use of laser scanning to detect fire-damaged concrete as a non-destructive technique by employing intensity image classification and analysis, relating intensity to concrete strength as well as assessing the difference between heated and unheated concrete. The experimental procedure for the proposed laser scanning technique for detecting fire-damaged concrete are explained in detail. The results of this technique are presented to demonstrate the feasibility and validity of the method.

2. EXPERIMENTAL PROCEDURE

2.1 Material and Test Specimens

Composite Portland cement, natural siliceous river sand (fine aggregate) and crushed siliceous coarse aggregate were used to create the concrete specimens. A water cement ratio of 0.44 was used. Prismatic beams of dimensions 400 x 100 x 100mm were prepared for normal strength concrete at the beginning of the project. The concrete mix proportion and properties are given in Table 1. This is a generic mix which is meant to represent many of the concrete structures, hence adding realism to the experiments.

Table 1: Material and Properties of Concrete Specimens

MATERIAL	WATER, SAND, AGGREGATE AND COMPOSITE PORTLAND CEMENT
Mix Proportions	0.44:1:1.42:3.17 (Water/cement/sand/aggregate)
Water–Cement ratio	0.44
Specimen size (Prismatic beams)	400mm X 100mm X 100mm
Curing Period	58days

The concrete specimens were removed from the moulds after 24 hours of casting and then cured in a fresh water tank for a period of 58 days. After curing, the concrete specimens were then stored in air with controlled relative humidity and temperature prior to scanning them. Since the same size of concrete specimens had to be scanned before and after heating they were then cut into half (i.e. 200 x 100 x 100mm) due to space limitation in the furnace.

2.2 Scanning Room and Instruments Used

The experiments were conducted under controlled laboratory conditions. The factors affecting the returned intensity under such conditions are the scanning geometry and the instrumental effetcs. The FARO Focus^{3D} 120 and the Leica HDS7000 laser scanners were used to scan the concrete specimens before and after heating. Below are the technical specifications of the scanners that were used (Table 2).

Table 2: Specification of TLS Instrument

Instrument	FARO Focus^{3D} 120	Leica HDS7000
Ranging method	Phase	Phase
Wavelength	905nm	1500nm
Field of View (Ver/Hor)	300˚ x 360˚	320˚ x 360˚
Laser Class	3R	1
Range	0.6-120m	0.3-187m
Samples/sec	976000	1016000
Beam diameter	Typical 3mm @ exit, circular	~3.5mm @ 0.1m
Beam divergence	Typical 0.19 mrad	< 0.3 mrad
Temp Range	5-40˚C	0-45˚C

Source: FARO Technologies (2011) and Leica Geosystems (2012)

2.3 Experiment Setup

The concrete blocks were placed on a steel frame at roughly the same height as the scanner to ensure normal incidence of the laser (shelf A in Fig. 1) and the scanning distance was 3 metres. In terms of the scanning geometry the incidence angle and the range affect the individual point signal to noise ratio (Soudarissanane *et al.*, 2011). The backscattered laser intensity decreases with respect to an increase in incidence angle and the range (Kaasalainen *et al*., 2011). Bitenc *et al.* (2010) state that the random range error taken from specifications is valid when the laser beam falls perpendicular to the target. In practice, the incidence angle is changing over the acquisition area and is usually non-perpendicular. The range error (δR) due to the non-perpendicular scanning geometry and the influence of δR on vertical and horizontal laser point positioning error is illustrated in Fig. 1 in the case of scanning the block on shelf B.

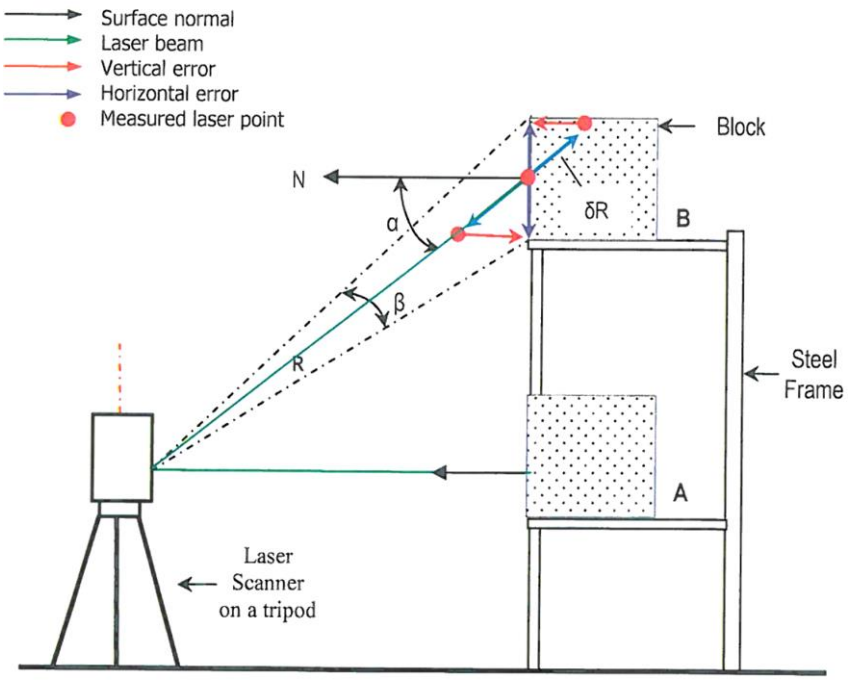

Fig. 1: Scanning the block at normal incidence and the range error at non-normal incidence. Modified from Bitenc *et al.* (2010).

High incidence angles result in poor intersection geometry and affect the range measurement precision. Bitenc *et al.* (2010) used a pulse laser scanner and calculated the range error as shown in Eq. (1) below where R denotes the range, β the beam divergence and α, the incidence angle.

$$\delta R = \frac{R.\beta .\tan \alpha}{2} \quad [1]$$

In this study the scanning distance only had an error of a few millimetres because an effort was made to scan as close as possible perpendicular to the concrete specimens.

2.4 Data Acquisition / Scanning Parameters

The scanning parameters used in the experiments are as follows: 1/5 resolution and a quality of 4X for the Faro scanner whereas super high resolution and normal quality for the HDS7000 scanner. The scanners used in the experiments have touch screen operations with intuitive interfaces which was helpful during the measurement setup. The FARO scanner's accuracy of the dual axis compensation is specified for inclinations up to 5° and will degrade above 5° (FARO Technologies, 2011). Efforts were made to level the scanner with an inclination less than 5° using the inclinometer screen and the clear contour filter was enabled in the scanner hardware in order to remove incorrect measurements at the edges of concrete specimens resulting from hitting two objects with the laser spot and mainly happens at the edges of the scanned objects. The HDS7000 scanner is a survey grade scanner and effective use of the digital bubble was made to accurately level the instrument through out the data aquisition session.

2.5 Thermal Treatment

After scanning the unheated concrete specimens with the laser scanner, the specimens had to be heated. A Carbolite CWF 12/23 electric furnace (Fig. 2) was used for the thermal treatment of the specimens. It is worth mentioning that the furnace used in this study is not a typical high end furnace used in civil engineering. The specimens were placed in the furnace chamber and thereafter heated at designated temperatures of 250, 400, 700, and 1000°C with a ramping rate of 10°C/min. The peak temperatures were maintained for 1 hour (fire exposure time) and after that time, the furnace was switch off with the specimen inside and left to cool down to room temperature in order to avoid thermal shock. For comparison purpose with the other heated specimens, one specimen was left unheated.

Fig. 2: Carbolite Furnace, shown is the outside and the chamber with a concrete block inside

3. DATA PROCESSING

3.1 Scan Data Pre-processing

The FARO scans were converted to text files (.pts) format using the FARO Scene sofware whereas the HDS7000 scans were to text files as well using the Z + F laser control software instead of the Leica Cyclone software as it has been reported for instance in Kaasalainen *et al*. (2011) that this software scales the intensity so as to accentuate visualisation. The scans which were converted to text files contained the geometric data in terms of X, Y and Z coordinates in a Cartesian coordinate system as well as radiometric data i.e. the intensity values for the 3D coordinates. The intensity values of data converted to text files were ranging from -2047 to +2048. The output Cartesian coordinates can be converted to spherical (range, zenith and azimuth angles) coordinates based on a zero origin for the TLS instrument as described in Eq. (2) (Soudarissanane *et al.*, 2009).

$$\begin{bmatrix} p_i \\ \theta_i \\ \phi_i \end{bmatrix}_{i=1....n} = \begin{bmatrix} \sqrt{x_i^2 + y_i^2 + z_i^2} \\ \tan^{-1}\left(\frac{y_i}{x_i}\right) \\ \tan^{-1}\left(\frac{z_i}{\sqrt{x_i^2+y_i^2}}\right) \end{bmatrix}_{i=1.....n} \quad [2]$$

For each block statistics such as intensity means and standard deviations were then calculated. Furthermore, intensity images were created using intensity data for the heated concrete blocks which was the followed by image classification.

3.2 Image Classification Procedure

The image classification procedure (Fig. 3) employed involved first creating a 2D intensity image, secondly generation of signature files and thirdly running the unsupervised classification using the maximum likelihood classifier. These procedural steps are explained in detail in the subsequent sections below.

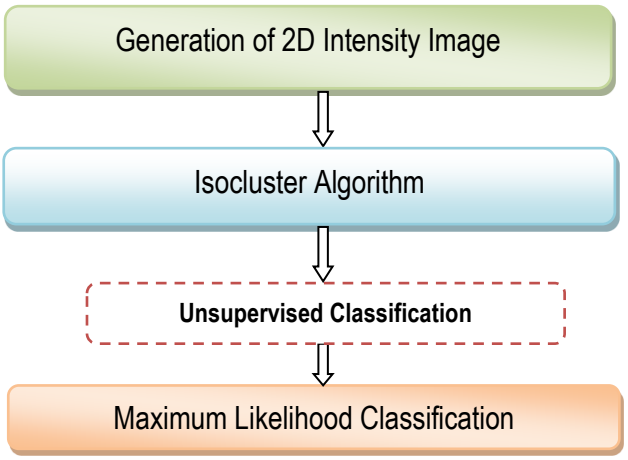

Fig. 3: Image Classification Procedure

3.2.1 Unsupervised Classification

According to Lillesand *et al.* (2008), unsupervised classification is where the outcomes (groupings of pixels with common characteristics) are based on the software analysis of an image without the user providing sample classes. The computer uses techniques to determine which pixels are related and what classes belong together. The Iso Cluster unsupervised classification algorithm (section 3.2.3) implemented in the ArcGIS software (ver. 10.2.2) was used for the intensity image classification.

3.2.2 ISO Cluster Algorithm

This algorithm uses an isodata clustering algorithm to determine the characteristics of the natural groupings of cells in multidimensional attribute space and stores the results in an output ASCII signature file (ESRI, 2012). The measure of similarity used to decide whether a pixel belongs to a particular class is the Euclidean distance (Armesto-González *et al.*, 2010).

$$\mathrm{d}_{a,b} = \sqrt{\sum_{i=1}^{m}(DN_a - DN_b)^2} \qquad [3]$$

Where $d_{a,b}$ indicates the distance between two pixels a and b, DN_a and DN_b are the digital numbers of these pixels. This algorithm proceeds according to the following steps (Armesto-González *et al.*, 2010):

i. Define the class centres, according to the number of clusters specified by the user.
ii. Assign all pixels in the image to the nearest class centre using the distance criterion.
iii. Calculate new class centres, taking into consideration the values of all pixels that were incorporated in the previous stage.
iv. Arrange the class centres depending on the parameters of control (for instance, the number of clusters).
v. Reassign all pixels of the image to the nearest centre.
vi. If the number of pixels that have switched clusters is lower than the number indicated by the user or if the maximum number of iterations is reached, then the process ends; if neither of these conditions is met, return to step (iii).

3.2.3 ISO Cluster Unsupervised Classification

This performs unsupervised classification on a series of input raster bands using the Iso Cluster and Maximum Likelihood Classification tools. This algorithm is implemented in the ArcGIS software (ver. 10.2.2) and combines the functionalities of the Iso Cluster and Maximum Likelihood Classification tools. It outputs a classified raster and it optionally outputs a signature file. The minimum valid value for the number of classes is two. There is no maximum number of clusters, although more clusters require more iterations. To provide the sufficient statistics necessary to generate a signature file for a future classification, each cluster should contain enough cells to accurately represent the cluster (ESRI, 2012).

4. RESULTS AND ANALYSIS

4.1 Visual Inspection of Concrete Intensity Images

Visual inspection is normally the initial step in the assessment of fire-damaged concrete. Fig. 4 shows the HDS7000 scanner intensity images of the concrete data based on the multi-hue colour scheme. The concrete intensity images show remarkable differences of the blocks that were heated to various temperatures and this is useful in roughly assessing the change in state of heated concrete which can then be supported by detailed investigations.

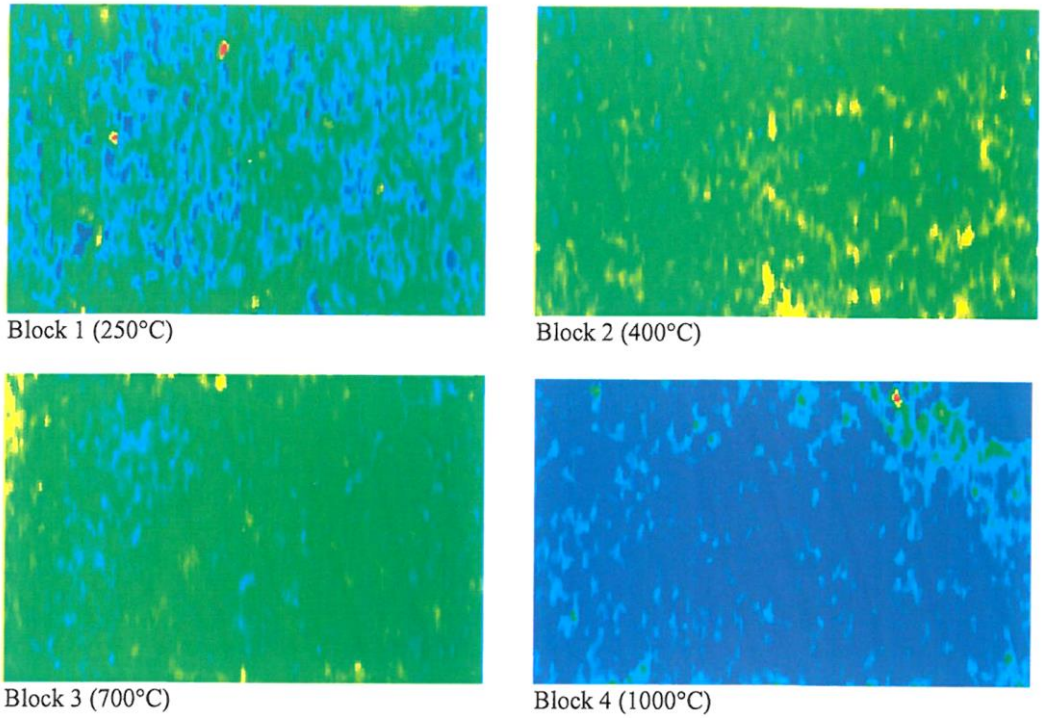

Fig. 4: Intensity images of heated concrete

4.2 Segmentation and Iso Cluster Unsupervised Classification

As explained above an unsupervised classification was employed using the Iso cluster algorithm and the maximum likelihood classifier. The classification was applied to the concrete intensity image for the block that was heated to a temperature of 1000°C in an effort to identify the physical modification of the block in terms of areas where cracks where prevalent. Segementation was also applied by manually and interactively thresholding the intensity above and below some user-defined bounds. Shown below are the results from the segmentation (Fig. 5a) and unsupervised classification (Fig. 5b). The areas where cracks were more pronounced are coloured white for segmentation and blue for unsupervised classification.

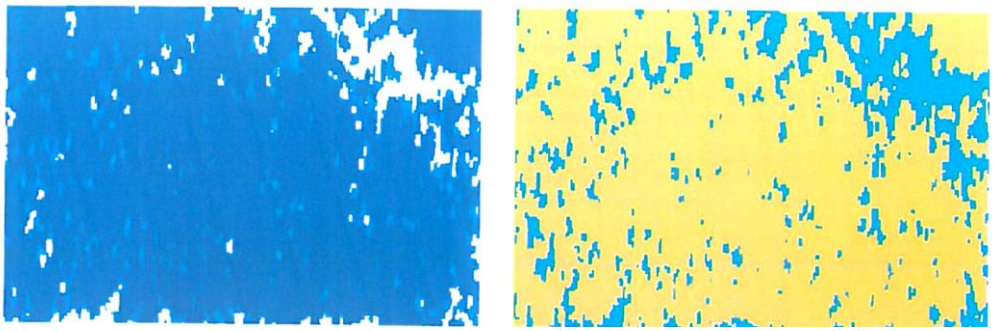
Fig. 5a: Segmentation

Fig. 5b: Unsupervised Classification

4.3 Concrete Strength Degradation

Compressive testing of the heated concrete blocks was conducted as shown in Fig. 6a and the relative compressive strength values of the concrete specimens after temperature exposure are presented in Fig. 6b. The relative strength was calculated as the percent retained strength of concrete with respect to the strength of the unheated concrete specimen. The relative strength of concrete significantly decreased after heating the blocks to the various temperatures. Between a temperature range of 250°C to 1000°C, the concrete strength degraded from 49 to 4% of orginal strength of unheated concrete.

Fig. 6a: Compressive Strength Testing

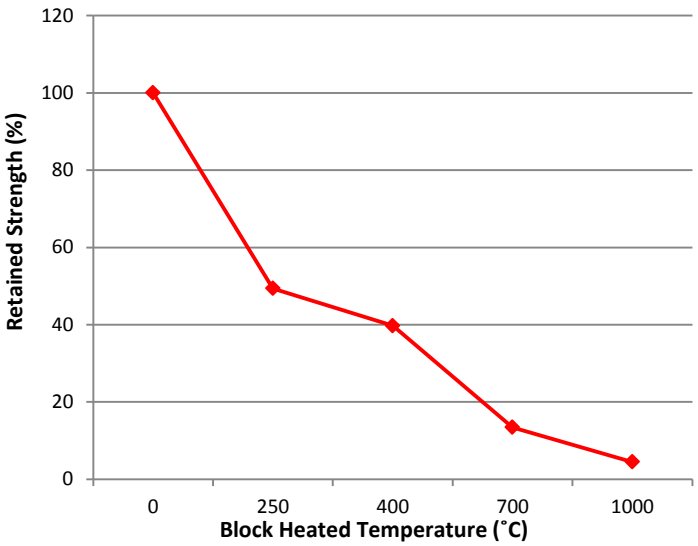

Fig. 6b: Retained Strength vs Block Heated Temperature

4.4 Relation of Intensity and Concrete Strength

The relationship between intensity and the retained strength of concrete is presented in Fig. 7 and it can be seen that the intensity increases with a decrease in the retained strength of the blocks which occurs when concrete is heated to elevated temperatures. Block C which acted as a control block has its strength intact as it was not heated. However, the intensity for this block is low compared to all other blocks (i.e block 1 to block 4) whose intensity increase with an increase in their exposure temperature which ranged from 250°C to 1000°C.

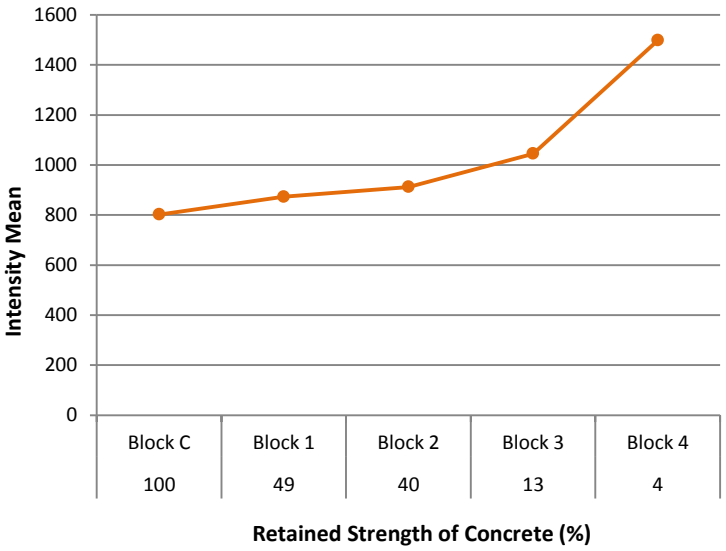

Fig. 7: Intensity vs retained Strength of heated concrete

4.5 Comparison of Unheated and Heated Concrete

The intensities of the concrete blocks before and after heating were compared with the aim of assessing if there were any differences and trends that could be observed in relation to the exposure temperature that each block was heated to. The results of the comparative analysis are shown in Fig. 8 and it can be observed that the intensity values of the blocks increase after heating and with an increase in exposure temperature.

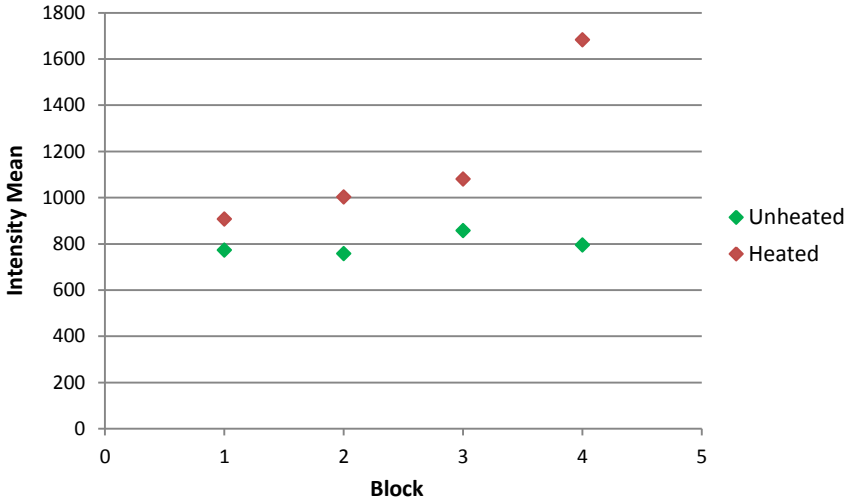

Fig. 8: Comparison of Unheated and Heated Concrete. The Blocks were heated as follows: Block 1 (250°C), Block 2 (400°C), Block 3 (700°C) and Block 4 (1000°C).

4.6 Difference between Unheated and Heated Concrete: Statistical Testing

Statistical testing involving the paired t-test was carried out to test for a statistical difference between the unheated and heated concrete blocks. A typical example of paired data includes before and after measurements as done in this study where scanning was conducted before and after heating the concrete blocks. Reasonable sizes of sections of the concrete specimens were used for the test so as to have more redundancy. Below is the paired t-test and results (Table 3) for the concrete specimens:

Hypothesis test for a paired t-test:
H_0: $\mu_d = \mu_0$ versus H_1: $\mu_d \neq \mu_0$

Where μ_d is the population mean of the differences and μ_0 is the hypothesized mean of the differences.

Table 3: Paired T-test results for heated and unheated concrete, FARO scanner

Block	*Condition*	*Sample #*	*Mean*	*StDev*	*SE Mean*
Block 1 (250°C)	Heated	3646	906.92	71.90	1.19
	Unheated	3646	824.67	71.31	1.18
	Difference	3646	82.25	100.36	1.66
	95% confidence interval for mean difference: (78.99, 85.51) T-Test of mean difference = 0 (vs ≠ 0): T-Value = 49.49, P-Value = 0.000				
Block 2 (400°C)	Heated	3725	1002.61	85.71	1.40
	Unheated	3725	834.03	73.38	1.20
	Difference	3725	168.58	106.87	1.75
	95% confidence interval for mean difference: (165.15, 172.02) T-Test of mean difference = 0 (vs ≠ 0): T-Value = 96.28, P-Value = 0.000				
Block 3 (700°C)	Heated	3545	1080.90	126.02	2.12
	Unheated	3545	835.97	74.25	1.25
	Difference	3545	244.93	143.97	2.42
	95% confidence interval for mean difference: (240.19, 249.67) T-Test of mean difference = 0 (vs ≠ 0): T-Value = 101.29, P-Value = 0.000				
Block 4 (1000°C)	Heated	3557	1681.62	106.72	1.79
	Unheated	3557	780.29	104.76	1.76
	Difference	3557	901.33	147.41	2.47
	95% confidence interval for mean difference: (896.48, 906.17) T-Test of mean difference = 0 (vs ≠ 0): T-Value = 364.67, P-Value = 0.000				

With reference to Table 3 above, the confidence intervals for the mean differences for all the blocks 1 to 4 do not include zero, which suggested a difference for each block before and after heating. The small p-value (p = 0.000) for all the blocks further suggested that the data are inconsistent with the null hypothesis that there is no difference. Since the p-values of the test statistics for all the concrete blocks were less than the chosen alpha level of 0.05, the null hypothesis was rejected for each test and it was therefore concluded that there is a statistically significant difference before and after

heating the concrete blocks and that laser scanning intensity data is capable of detecting the difference.

5. DISCUSSION AND CONCLUSION

A method that employs laser scanning for detection of fire-damaged concrete was investigated and the following main points can be drawn from the study:

i. Intensity image analysis is a valuable factor in visual inspection of fire-damaged concrete and in the assessment of concrete physical changes due to heating.
ii. The relative strength of concrete reduced with an increase in exposure temperature whereas the intensity increased with a decrease in the strength of concrete. High intensity therefore implies a reduction in compressive strength of concrete.
iii. Heated concrete has higher intensity return compared to unheated concrete and this implies that laser intensity can be used to distinguish heated from unheated concrete.
iv. In spite of the good results achieved in this study of a promising detection technique for fire-damaged concrete conducted under controlled laboratory conditions and the scanning geometry optimsed, laser intensity correction is needed before applying the method in real life situations where the factors that affect the intensity return cannot be controlled and where scanning is not usually done perpendicular to the target.

REFERENCES

Armesto-González, J, Riveiro-Rodríguez, B, González-Aguilera, D and Rivas-Brea, M.T (2010) Terrestrial laser scanning intensity data applied to damage detection for historical buildings. Journal of Archaeological Science. 27, 3037-3047.

Arioz, O. (2007) Effects of elevated temperatures on properties of concrete. Fire Safety Journal 42 (8) 516-522.

Bitenc, M, Lindenbergh, R, Khoshelham, K and vanWaarden, A.P. (2010) Evaluation of a laser land-based mobile mapping system for monitoring sandy coasts. International Archives of Photogrammetry, Remote Sensing and Spatial Information Sciences, 38 (Part 7B) (2010), pp. 92–97.

Ergün, A, Gökhan, K, Serhat, B.M and Mansour, M (2013) The Effect of Cement Dosage on Mechanical Properties of Concrete Exposed to High Temperatures. Fire Safety Journal, 55, 160-167.

ESRI (Environmental Systems Research Institute) (2012) ArcGIS Help 10.1 (on-line) http://resources.arcgis.com/en/help/main/10.1. Accessed on 31st December 2015.

FARO Technologies (2011) FARO Laser Scanner Focus^{3D} User Manual.

Felicetti, R (2013) Assessment Methods of Fire Damages in Concrete Tunnel Linings. Fire Technology, 49 (2) 509-529.

Gosain, N.K, Drexler, R.F, and Choudhuri, D. (2008) Evaluation and Repair of Fire-Damaged Buildings, Structural Forensics - Investigating Structures and their Components (on-line) http://www.structuremag.org/wp-content/uploads/2014/08/C-STRForensics-Fire-Gosain-Sept081.pdf, accessed on 12.05.2014.

Hancock, C. M, Roberts, G.W, Bisby, L, Cullen, M and Arbuckle, J (2012) Detecting Fire Damaged Concrete Using Laser Scanning. FIG Working Week, Rome, Italy, 6-10 May.
Ingham, J. (2009) Forensic Engineering of Fire-damaged Structures, Proceedings of Institution of Civil Engineers, 162, CE5.
Kaasalainen, S, Jaakkola, A, Kaasalainen, M, Krooks, A and Kukko, A (2011) Analysis of Incidence Angle and Distance Effects on Terrestrial Laser Scanner Intensity: Search for Correction Methods. Remote Sensing, 3, 2207-2221.
Leica Geosystems (2012) HDS7000 User Manual (on-line) http://hds.leica-geosystems.com, accessed on 14th July 2014.
Lillesand, T. M., Kiefer, R. W. and Chipman, J. W. (2008) Remote Sensing and Image Interpretation, Sixth Edition, John Wiley and Sons, New Jersey.
Short, N. R., Purkiss, J. A and Guise, S. E. (2001) Assessment of Fire Damaged Concrete using Colour Image Analysis. Construction and Building Materials, 15 (1), 9-15.
Soudarissanane, S., Lindenbergh, R., Menenti, M. and Teunissen, P. (2009) Incidence Angle Influence on the Quality of Terrestrial Laser Scanning Points. International Archives of the Photogrammetry, Remote Sensing and Spatial Information Sciences, 38 (3/W8), 183-188.
Soudarissanane, S, Lindenbergh, R, Menenti, M. and Teunissen P. (2011) Scanning Geometry: Influencing Factor on the Quality of Terrestrial Laser Scanning Points. ISPRS Journal of Photogrammetry and Remote Sensing, 66 (4) 389-399.

BIOGRAPHICAL NOTES

Mr. Mukupa is a post graduate research student in the Department of Civil Engineering at The University of Nottingham, Ningbo, China. He is currently pursuing a PhD in Engineering Surveying.

Prof. Roberts is a Professor in Geospatial Engineering at The University of Nottingham, Ningbo, China. He is the UN Delegate for the FIG through the Chartered Institution of Civil Engineering Surveyors. He has co-authored over 200 papers and he is a past chairman of FIG Commission 6.

Dr. Hancock is a Lecturer (Assistant Professor) at The University of Nottingham, Ningbo, China. He is also involved with the International Federation of Surveyors (FIG) and has been a Vice Chair for communications on Commission 6 (Engineering Surveys) from 2010 – 2013.

Dr. Al-Manasir is a Lecturer (Assistant Professor) at The University of Nottingham, Ningbo, China since September 2012. Before joining UNNC, he worked as an Assistant Professor of Geomatics in Jordan from September 2009 to August 2012. He also served as laser scanning specialist and as acting manager for aerial mapping at Limitless LLC.

CONTACTS

Mr. Wallace Mukupa
The University of Nottingham, Ningbo, China.
Faculty of Science and Engineering

Department of Civil Engineering
199 Taikang East Road
Ningbo 315100
CHINA
Tel. +86 (0) 574 8822 2623
Email: wallace.mukupa@nottingham.edu.cn
Web site: www.nottingham.edu.cn